Cerium doped hydroxyapatite nanoparticles synthesized by coprecipitation method

CARMEN STELUTA CIOBANU[1,2], CRISTINA LIANA POPA[1] AND DANIELA PREDOI[1]*

[1]National Institute of Materials Physics, P.O. Box MG 07, 07725, Magurele, Romania;

[2]University Politehnica of Bucharest, Faculty of Applied Chemistry and Materials Science, Department of Science and Engineering of Oxide Materials and Nanomaterials, 1-7 Polizu Street, P.O. Box 12-134, 011061 Bucharest, Romania.

[*]corresponding author: dpredoi@gmail.com

Abstract: The present work reports a simple coprecipitation adapted method for the synthesis of stable Ce substituted to Ca hydroxyapatite nanoparticles. The structural and morphological properties of Ce doped hydroxyapatite (Ce:HAp) were characterized by X-ray diffraction (XRD), Scanning Electron Microscopy (SEM) and Energy Dispersive X-ray analysis (EDAX). The optical properties of Ce doped hydroxyapatite were also investigated using Fourier Transform Infrared (FTIR) spectroscopy, FT Raman spectroscopy and photoluminescence analysis. The results of the XRD studies revealed the progressive increase in the a- and c-axes with increasing of Ce concentrations. The nanometric dimensions of the particles were also confirmed by the SEM micrographs. In the FTIR studies of Ce:HAp powders a similar structure to hydroxyapatite was observed. IR and Raman wavenumbers and the peak strength of the bands associated to the P-O and O-H bonds decreases progressively with the increase of Ce concentration. The results obtained by FTIR and Raman spectroscopies confirmed the XRD analysis. All the emission maxima could be attributed to the 5d-4f transitions of Ce ions. The displacement of maximum emission bands with the increase of Cerium in the samples is in agreement with the results obtained by XRD studies.

Keywords: *biomaterials; FTIR; FT Raman; photoluminescence.*

RUNNING TITLE: CERIUM DOPED HYDROXYAPATITE NANOPARTICLES

INTRODUCTION

Hydroxyapatite is one of the most studied biomaterial with chemical formula $Ca_{10}(PO_4)_6(OH)_2$, (HAp) and represents the principal inorganic component of bones and teeth.

Its excellent biological properties (biocompatibility, osteoconductivity, inductivity, etc.) have made HAp a suitable material for the biomedical field.[1-6] Recent studies have demonstrate that the structure of apatite allows a large number of substitutions.[7-9] These substitutions modify the physical, chemical and biological properties of HAp. Moreover, the crystallinity, solubility and thermal stability are also influenced by the substitution of Ca with different ions (Eu, Ag, Sm, Zn, Cu etc.). The substitution of Ca with Ce is also possible due to the fact that their radius and electronegativity are almost equal.

Studies conducted by Doat et al. have shown that lanthanide-doped hydroxyapatite (eg: europium doped hydroxiapatite) nanoparticles can be used as bioactive fluorescent carriers of biological molecules and drugs. [10-12]

It is well known that the morphology, structure and the physicochemical properties of HAp powders depend on the synthesis method. In order to synthesize hydroxyapatite nanopowders various techniques such as precipitation, sol–gel, solid-state reactions, pyrolysis, microwave synthesis, mechanochemical route can be used.[13-14]

It has been found that in the human body, cerium (Ce) can act similarly to calcium and accumulate in bones. According to these results, Cerium doped hydroxyapatite could improve/stimulate the metabolism.[15-16] On the other hand, Cerium ions also have antimicrobial activity and unique regenerative properties. Moreover, recent studies have shown that the use of Cerium in dentistry may help prevent cavities.[17-18] These biological properties make Cerium suitable for applications in biomedical field.[19]

A large number of studies are also conducted in order to discover new biomaterials with improved biological and physicochemical properties (especially antibacterial and luminescent) in order to be successfully used in the biomedical field.

Due to the fact that Ce cations possess luminescent properties (under UV excitation)[20-21] and antimicrobial activity, their incorporation in the HAp structure can conduct to obtaining a biomaterial with promising applications in medicine (for imaging, drug delivery, etc.).

The present structural, morphological and optical studies are conducted on synthesized $Ca_{10-x}Ce_x(PO_4)_6(OH)_2$; called here Ce:HAp, with small concentrations of incorporated Cerium (x_{Ce} = 0.01, 0.03, 0.05) in the hydroxyapatite structure in order to demonstrate that the Ca is replaced by Ce in the apatite lattice. The structural changes to the apatite lattice after Ca substitution by Ce at small concentrations is described here for the first time. All Ce:HAp

samples were characterized by X-ray diffraction (XRD), Scanning Electron Microscopy (SEM), Energy Dispersive X-ray analysis (EDAX), Fourier Transform Infrared (FTIR) spectroscopy, FT Raman spectroscopy and photoluminescence analysis. This study proposes various complementary characterization techniques for a general understanding of what happens in the apatite lattice when Ca is replaced by Ce.

EXPERIMENTAL

Powders preparation

In this work, Ce doped $Ca_{10}(PO_4)_6(OH)_2$ powders- ($Ca_{10-x}Ce_x(PO_4)_6(OH)_2$; Ce:HAp) with different concentrations of Cerium (x_{Ce} = 0.01, 0.03, 0.05) have been synthesized by coprecipitation method. To prepare Ce:HAp nanoparticles by coprecipitation method, an aqueous solution of $(NH_4)_2HPO_4$ was slowly added to an aqueous solution containing cerium nitrate and calcium nitrate tetrahydrate $Ca(NO_3)_2{\cdot}4H_2O$ upon continuous stirring. The pH of the mixture was adjusted to 10 by adding NH_4OH and the reaction temperature was maintained at 100 ℃. The resulting precipitate was washed with deionised water and then filtered. The powder was dried at 100 ℃ for 48h.

Powders characterisation

The powders were investigated by X-ray diffraction using a Bruker D8 Advance diffractometer, with nickel filtered Cu K_α (λ = 1.5418 Å) radiation, and a high efficiency one-dimensional detector (Lynx Eye type) operated in integration mode. The diffraction patterns were collected in the 2θ range 20 º – 60 º, with a step of 0.02 º and 34 s measuring time per step. Insightful analyses of the Ce:HAp structures, were carried out by Rietveld refinement analysis using the MAUD code.[22-23] Scanning electron microscopy (SEM) measurements were performed using a Quanta Inspect F microscope from FEI Company, equipped with an energy-dispersive X-ray spectrometer (EDAX). The FTIR studies of the powders were performed using a Spectrum BX Spectrometer. The specimens were prepared as following: 1 % of the powder was mixed and grounded with 99 % KBr. Tablets of 10 mm diameter were obtained by pressing the powder mixture at a load of 5 tons for 2 min. The spectrum was registered in the spectral region 400 - 4000 cm^{-1} with resolution 4 cm^{-1} and 128 scans. FT Raman Bruker RFS 100 spectrophotometer was used in order to obtain complementary information about optical properties about Ce:HAp powders. The powders were excited using a laser wavelength excitation of 1064 nm. The spectra were recorded with a resolution of 4 cm^{-1} and 100 scans. The

fluorescence emission spectra were obtained by using a HORIBA Scientific Fluorolog-3 spectrofluorometer (model FL3-2iHR320 with Hamamatsu R-928 PMT).

RESULTS AND DISCUSSIONS

The X-ray diffraction patterns of cerium doped hydroxyapatite, $Ca_{10-x}Ce_x(PO_4)_6(OH)_2$, with different concentrations of cerium (x_{Ce} = 0.01, 0.03, 0.05) are depicted in Fig. 1A. The broad peaks in the X-ray diffraction patterns assigned to the characteristic planes (0 0 2), (2 1 0), (2 1 1), (3 0 0), (2 0 2), (3 1 0), (2 2 2), (1 2 3) and (0 0 4) of $Ca_{10-x}Ce_x(PO_4)_6(OH)_2$ (x_{Ce} = 0.01, 0.03, 0.05) are in accordance with the expected patterns for crystalline hydroxyapatite with hexagonal structure (JCPDS No. 9-432). In these diffraction patterns were not observed separate phases for cerium oxide or other impurity phases. Nevertheless, when some Ca sites are replaced by Ce, there is a tendency of distorting the lattice cell parameters. For the peaks registered at lower degrees, a slight shift was observed. This behaviour seems to be the effect of substitutions that change the crystal structure (Fig. 1B), which according to P.N. Lim *et al.*[24] suggests a significant incorporation of the dopants into the apatite lattice. The crystallite sizes of all the Ce:HAp samples decreased with the increase of Ce concentration in the samples (Table 1). In this study, both the a- and c-axes increased with the increase of Ce substitutions (Table 1). This result is logical because the ionic radius of Ce (0.107 nm) is greater than to the ionic radius of Ca (0.100 nm) and packaging of the larger size atoms has the tendency to distort the lattice parameters.[25-26]

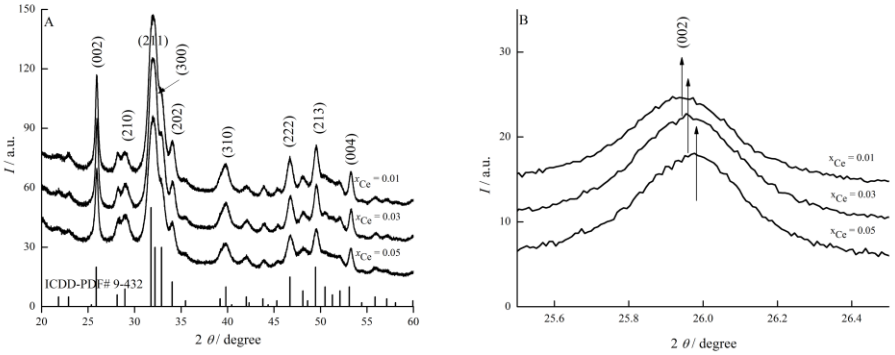

Fig. 1. (A) X-ray diffraction patterns of Ce:HAp with x_{Ce} = 0.01, 0.03, 0.05.
(B) X-ray diffraction patterns comparison between Ce:HAp with x_{Ce} = 0.01, 0.03, 0.05.

These results obtained from XRD studies demonstrate that the Ce:HAp powders synthesised by adapted coprecipitation method revealed the characteristic structure of

hydroxyapatite with good crystal structure without finding the presence of any new phase or impurity.

TABLE 1. Lattice cell parameters and the crystallite sizes of $Ca_{10-x}Ce_x(PO_4)_6(OH)_2$ obtained from Rietveld refinement.

Samples Ce:HAp	Cell parameters		Crystallite sizes, nm
	a /nm	*c* /nm	
x_{Ce} = 0 (JCPDS 9-432)	0.9418	0.6884	
x_{Ce} = 0.01	0.9420 ± 0.0001	0.6886 ± 0.0001	25.45 ± 0.1
x_{Ce} = 0.03	0.9424 ± 0.0002	0.6889 ± 0.0003	22.86 ± 0.1
x_{Ce} = 0.05	0.9436 ± 0.0002	0.6895 ± 0.0004	18.95 ± 0.1

In order to examine the microstructure and elemental composition of Ce:HAp powders (with x_{Ce} = 0.01; 0.03; 0.05), scanning electron microscopy studies were performed. The SEM images and EDAX spectrum of Ce:HAp samples are presented in Fig. 2 (x_{Ce} = 0.01); Fig. 3 (x_{Ce} = 0.03) and Fig. 4 (x_{Ce} = 0.05). In the SEM images presented below it can be observed that the increase of Ce concentration slightly influences the morphology of the samples. Moreover, the ellipsoidal shape of nanoparticles is preserved for all the samples. The SEM micrographs confirmed the nanometric dimensions of the particles but also their tendency to agglomerate. This behavior (tendency to agglomerate) is owed most probably to the nanometric dimensions of the particles.

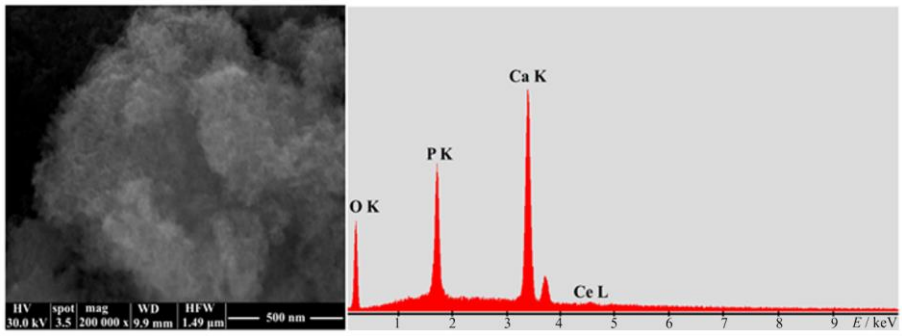

Fig. 2. SEM image and EDAX spectra of Ce:HAp (x_{Ce} = 0.01) powder.

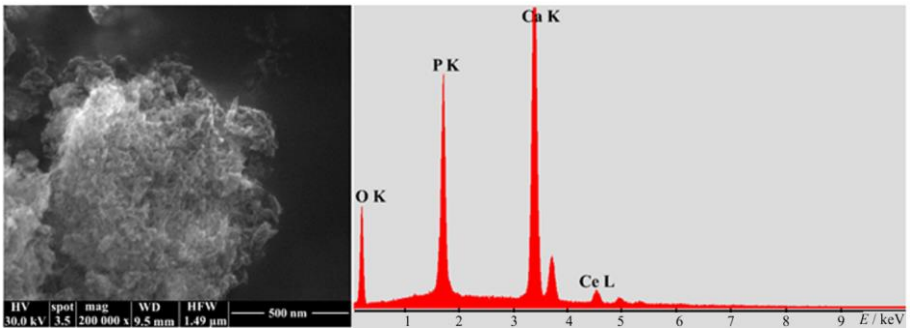

Fig. 3. SEM image and EDAX spectra of Ce:HAp (x_{Ce} = 0.03) powder.

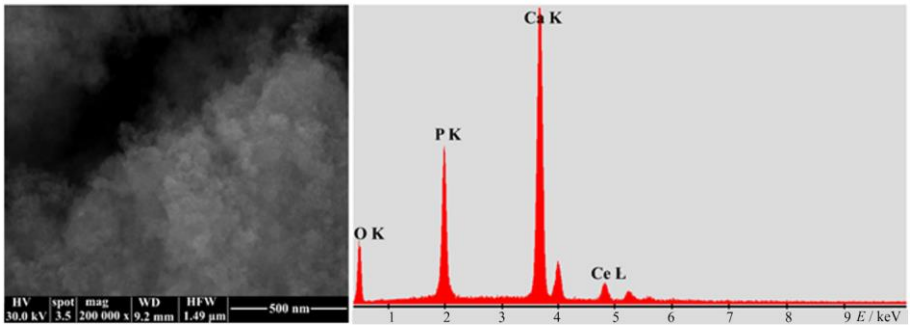

Fig. 4. SEM image and EDAX spectra of Ce:HAp (x_{Ce} = 0.05) powder.

The EDAX spectra of the studied powders have confirmed the presence of all constituent elements of Ce:HAp powders: Ce, Ca, P and O. On the other hand, these studies confirm the increase of Ce concentrations in the samples.

In the FTIR (Fig. 5) spectra of Cerium doped hydroxyapatite are presented the characteristic vibrational bands related to the phosphate, hydroxyl and adsorbed water. Moreover, the additional band attributed to carbonate group (1269 cm^{-1}) is also presented.

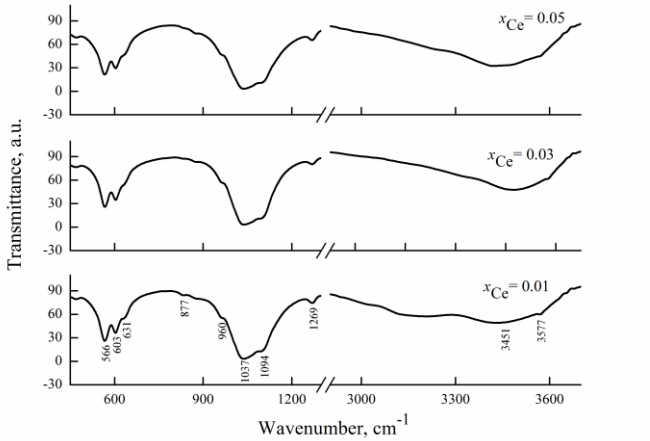

Fig. 5. FTIR spectra of cerium doped hydroxyapatite powders.

The vibrational bands from the region 3100-3460 cm^{-1} are attributed to the adsorbed water. The bands at 3577 cm^{-1} and 631 cm^{-1} are assigned to stretching and vibrational mode of hydroxyl group (OH^-).[27] The presence of the bands at 566, 603 (assigned to the ν_4 bending mode of PO_4^{3-} groups) and 631 cm^{-1} indicates the formations of a well crystallized powder.

Phosphate ν_1 stretching mode band is present at 960 cm^{-1} and PO_4^{3-} ν_3 stretching mode at 1094 and 1037 cm^{-1} respectively. On the other hand, the band at 470 cm^{-1} is assigned to ν_2 bending mode of PO_4^{3-} group. Furthermore, we can see that the IR wavenumber and the peak strength of P-O and O-H bonds decreased progressively with the increase of Ce concentrations.

Complementary information to those obtained by FTIR spectroscopy are obtained by Raman spectroscopy. The main vibrational bands observed in the Raman spectra (Fig. 6) are attributed to the stretching (ν_3 and ν_1) and bending (ν_4) modes of the phosphate group from the HAp structure. The bands from 594 and 610 cm^{-1} are assigned to the ν_4 bending mode of PO_4^{3-} group. On the other hand, phosphate ν_1 stretching mode band appears at 965 cm^{-1} and another stretching mode (ν_3) is observed at 1053 cm^{-1}.

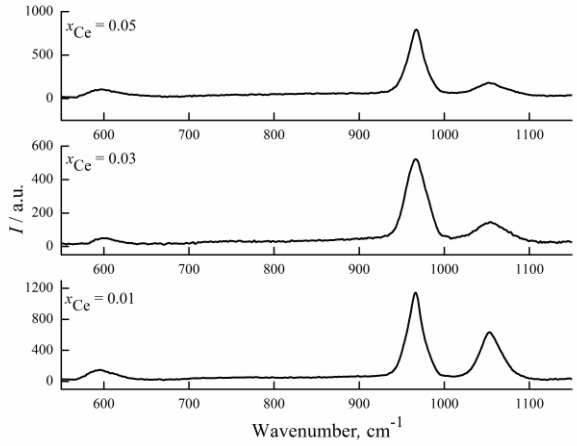

Fig. 6. Raman spectra of cerium doped hydroxyapatite powders.

In the Raman spectra we could also observe that the intensity of the vibrational bands decreased with the increase of Cerium concentration in the powders. This behaviour is due to the substitution of Ca ions with larger ions (Ce) in the HAp lattice which leads to a decrease of bonding strength of P-O.[21] These results obtained by Raman spectroscopy are in good agreement

with the information derived from the FTIR studies presented above. On the other hand, the results obtained by FTIR and Raman spectroscopies confirmed the XRD analysis.

The emission spectra of Ce:HAp samples with x_{Ce} = 0.01; 0.03 and 0.05 are presented in Fig. 7. Under an excitation of 250 nm, the spectrum (Fig. 7) has a maximum around 390 nm and a shoulder at about 350 nm which covers a wavelength range from 330 nm to 430 nm.

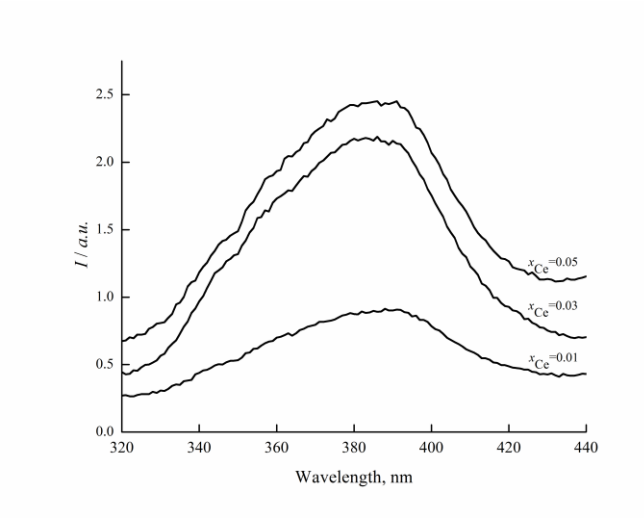

Fig. 7. Emission spectra of Ce:HAp (x_{Ce} = 0.01; 0.03 and 0.05) powders (λ_{exc} = 250 nm).

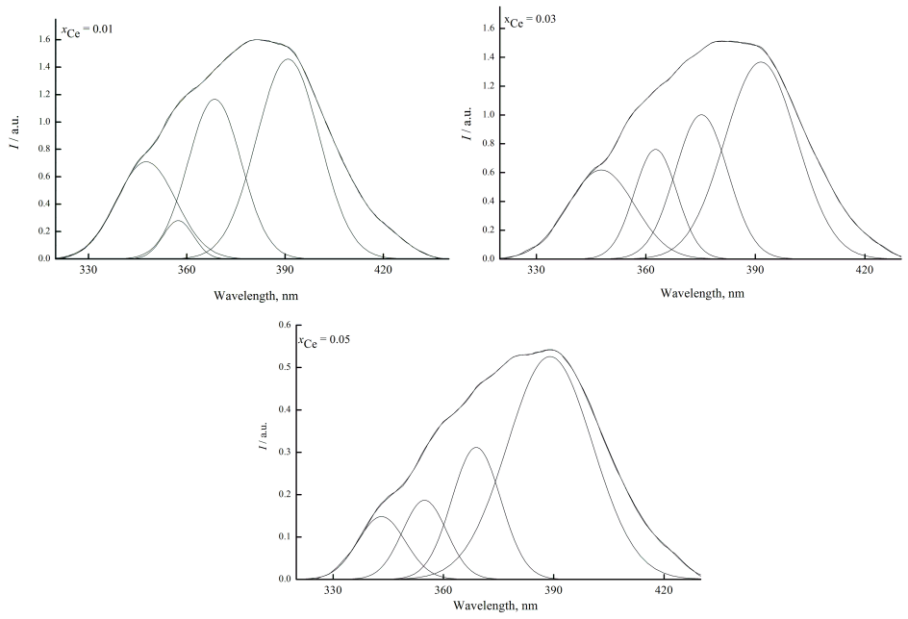

Fig. 8. Deconvolution of the emission spectra of Ce:HAp (x_{Ce} = 0.01; 0.03 and 0.05) powders (λ_{exc} = 250 nm).

Due to the fact that the spectra have an asymmetry, we deconvoluted them into four Gaussian peaks with maxima around: 390, 375, 357 and 347 nm (Fig. 8). All this emission maxima could be attributed to the 5d-4f transitions of Ce ions.

In the structure of HAp two types of Ca site (positions) are present: Ca (I) and Ca (II). Here, the emission maximum around 360 nm is attributed to Ce ion which substituted the Ca(I) position in the hydroxyapatite structure.[28] Moreover, the emission band at around 390 nm occurs due to Ce ion which substituted the Ca(II) position. The results reported in this paper are in good agreement with the data reported in the literature.[29] Furthermore, it is obvious that the intensity of the emissions bands increase with the increase of Cerium concentrations in the samples. Also, we observed the displacement of the maximum emission bands with the increase of Cerium in the samples. These results are in agreement with the results obtained by XRD studies.

CONCLUSIONS

In this article, the synthesis of hydroxyapatite doped with small concentration of cerium is reported. The lattice parameters have shown that Ce substituted Ca in the apatite structure. The crystal size decreased when the concentration of Ce increased. The results obtained in the XRD studies demonstrate that the Ce:HAp powders synthesized by an adapted coprecipitation method present the hydroxyapatite characteristics with good crystalline structure without any other new phases or impurities. Raman and FTIR studies confirmed the initial results obtained by XRD investigations. The deconvolution of the emission spectra of all Ce:HAp samples revealed four peaks that can be attributed to the 5d-4f transitions of Ce ions. In conclusion, the results presented in this paper encourage further studies and research on cerium doped hydroxyapatite for antimicrobial properties with possible applications as an antimicrobial agent.

Acknowledgements: The work has been funded by the Sectoral Operational Programme Human Resources Development 2007-2013 of the Ministry of European Funds through the Financial Agreement POSDRU/159/1.5/S/134398. We thank HORIBA Scientific and especially Dr. Reynald HURTEAUX and Dr. Patrick Chapon from Horiba Jobin Yvon SAS France for the access to their specific instrumentation.

REFERENCES

1. R. Gorcia, R. H. Doremus, *J. Mater. Sci. - Mater. Med*. **3** (1992) 154.
2. C. K. Hsu, *Mater. Chem. Phys.* **9470** (2002) 1.
3. T. Kokubo, *Bioceramics and Their Clinical Applications*, CRC Press, Boca Raton, Cambridge, UK, 2008.
4. J. Park, *Bioceramics: Properties, Characterizations and Applications*, Springer, New York, USA, 2008, p. 359.
5. S. V. Dorozhkin, *Calcium orthophosphates: applications in nature, biology and medicine*, Pan Stanford, Singapore, 2012, p. 850.
6. S. V. Dorozhkin, *J. Mater. Sci.- Mater. Med.* **24** (2013) 1335.
7. C. S. Ciobanu, C. L. Popa, D. Predoi, *J. Nanomat.* **2014** (2014) 1.
8. C. S. Ciobanu, F. Massuyeau, L. V. Constantin, D. Predoi, *Nanoscale Res. Lett.* **6** (2011) 613.
9. C. S. Ciobanu, S. L. Iconaru, F. Massuyeau, L. V. Constantin, A. Costescu, D. Predoi, *J. Nanomater.* **2012** (2012) 1.
10. S. P. Mondejar, A. Kovtun, M. Epple, *J. Mater. Chem.* **17** (2007) 4153.
11. P. Yang, Z. Quan, C. Li, X. Kang, H. Lian, J. Lin, *Biomaterials.* **29** (2008) 4341.
12. A. Doat, F. Pellé, N. Gardant, A. Lebugle, *J. Solid State Chem.* **177** (2004) 1179.
13. S. Koutsopoulos, *J. Biomed. Mater. Res.* **62** (2002) 600.
14. S. V. Dorozhkin, *Int. J. Chem. Mater. Sci.* **1** (2013) 105.
15. J. Emsley, *Nature's Building Blocks: An A–Z Guide to the Elements*, Oxford University Press, USA, 2011.
16. M. A. Jakupec, P. Unfried, B. K. Keppler, *Rev. Physiol. Biochem. Pharmacol.* **153** (2005) 101.
17. J. Hui, Z. Weipo, L. Huanhe, *Chin. J. Stomatology.* **32** (1997) 143.
18. X. F. Liu, M. J. Tu, *Modern Chemical Industry.* **25** (2005) 145.
19. Y. Lin, Z. Yang, J. Cheng, *J. Rare Earths.* **25** (2007) 452.
20. Z. Feng, Y. Liao, M. Ye, *J. Mater. Sci. - Mater. Med.* **16** (2005) 417.
21. L. Yingguang, Y. Zhuoru, C. Jiang, *J. Rare Earth.* **25** (2007) 452.
22. L. Lutterotti, *Nucl. Instr. Meth. Phys. Res.* **268** (2010) 334.
23. N. C. Popa, *J. Appl. Crystallogr.* **31** (1998) 176.
24. P. N. Lim, B. Y. Tay, C. M. Chan, E. S. Thian, *J. Biomed. Mater. Res. Part. B.* **100B** (2012) 285.
25. C. Ergun, T. J. Webster, R. Bizios, R. H. *J. Biomed. Mater Res.* **59** (2002) 169.
26. F. Miyaji, Y. Kono, Y. Suyama, *Mater. Res. Bull.* **40** (2005) 209.
27. I. V. Berezovskaya, N. P. Efryushina, G. B. Stryganyuk, A. S. Voloshinovskii, E. V. Zubar, V. P. Dotsenko, *Func. Mater.* **15** (2008) 164.
28. I. V. Berezovskaya, N. P. Efryushina, E. V. Zubar, V. P. Dotsenko, *Proceedings Of The International Conference Nanomaterials: Applications And Properties*, (2012), Sumy State University, Ukraine, 2012, Abstract No. 01PCN24.